

# Synthesis, Characterization, and Properties of Interpenetrating Polymer Networks Containing Functionalized Latex Particles

DOUGLAS J. HOURSTON,\* FRANZ-ULRICH SCHÄFER, and JOHN S. BATES

Institute of Polymer Technology and Materials Engineering, Loughborough University of Technology, Loughborough, LE11 3TU, United Kingdom

## SYNOPSIS

Three-component interpenetrating polymer networks (IPNs) comprising polyurethane (PUR), poly(*n*-butyl methacrylate) (PBMA), and polystyrene (PS) latex particles were prepared in a modified one-shot synthesis. The hydroxy-functionalized and unmodified polystyrene latex particles were synthesized via a seeded emulsion polymerization. The incorporation of hydroxyethyl methacrylate into the latex particles was confirmed via diffuse reflectance infrared analysis and modulated-temperature differential scanning calorimetry. The IPNs were characterized by dynamic mechanical thermal analysis, tensile testing, hardness measurements, and transmission electron microscopy. The three-component materials exhibited higher values for the Young's modulus and the Shore A hardness and for the dynamic storage modulus in the higher temperature range from 80 to 140°C than did the PUR/PBMA IPN alone. The latex particles with the hydroxyl functionality exhibited a better miscibility with the microheterogeneous PUR/PBMA IPN than did unfunctionalized PS latex particles, and, therefore, resulted in materials with better damping properties in the temperature range between 80 and 140°C. Transmission electron micrographs confirmed the improved miscibility of the functionalized latex particles. The latex particles were not, however, dispersed on an individual level but formed agglomerates of between 2 and 20  $\mu\text{m}$ . © 1996 John Wiley & Sons, Inc.

## INTRODUCTION

Interpenetrating polymer networks (IPNs) consist of two or more polymers of which at least one is crosslinked in the presence of the other network.<sup>1-3</sup> If interlocking of the chains precedes phase separation, a forced degree of mixing is obtained. This might result in materials with a microheterogeneous morphology exhibiting a broad glass transition region. Hence, one major potential application for IPNs is in the field of sound and vibration damping.<sup>4,5</sup> In real damping applications wide variations of temperature and frequency are experienced, thus requiring damping systems with a high and broad  $\tan \delta$  range.

Three-component IPNs have previously been synthesized by Klempner and Frisch<sup>6-8</sup> and by Wang et al.<sup>9</sup> Their simultaneous syntheses relied on three independent polymerization reactions, isocyanate and epoxy curing and a free radical reaction. In the present study, polystyrene (PS) latex particles were prepared first, and then mixed and reacted with the polyurethane precursors, the methacrylic monomer, and the crosslinker. Structured latex particles have been used for the toughening of homopolymers such as thermoplastic poly(methyl methacrylate)<sup>10</sup> and thermosets such as epoxy resins.<sup>11</sup> For this purpose, latex particles with a diameter<sup>11</sup> between 0.2 and 2  $\mu\text{m}$  with a low glass transition temperature ( $T_g$ ) core polymer are most commonly used. In the present study, glassy functionalized and unfunctionalized PS particles were incorporated into an elastomeric IPN.

The objective of this study was to develop materials that exhibit better mechanical properties at

\* To whom correspondence should be addressed.

high temperatures than the polyurethane (PUR)/poly(*n*-butyl methacrylate) (PBMA) two-component IPN. The latter is a good damping material with a high intrinsic energy-absorbing ability over a limited temperature/frequency range. The principal objective was to broaden further the damping temperature range by the incorporation of functionalized latex particles into the PUR/PBMA IPN. In addition to extending the transition region to higher temperatures, the PS latex particles should act as a polymeric filler in the IPN, since at the  $T_g$  of the PUR and the PBMA, the PS latex particles are still in the glassy state. Fillers are known to be able to broaden<sup>12,13</sup> the damping range and increase<sup>9,12,14</sup> the damping ability by introducing additional damping mechanisms. They can resonate<sup>15</sup> and/or reflect impinging sound waves back through the polymer. Also, energy can be converted<sup>12,13</sup> into heat through an increase in friction and shear in the system. This is achieved through particle-particle friction<sup>12</sup> in filler agglomerates, through particle-polymer friction, or through filler particles acting as mini-constrained layer<sup>13</sup> systems.

The composition range of the filler which will yield improved damping is likely to be limited by two factors. Too little filler will be ineffective, while too much will decrease the volume percentage of the IPN, so that the height of the  $T_g$  transition will be reduced and shifted out of the desired damping range. Increasing the damping ability through the creation of additional shear in the system and broadening the damping range might require different weight fractions of filler addition. While 7% has been found as an optimum<sup>9</sup> for the former, around 20% of a polymer is needed to observe an effect on the dynamic mechanical property profile. Thus, the PS composite latex particles were incorporated at 17 wt %. A 70 : 30 PUR/PBMA IPN composition was chosen because of the special properties found at this composition for many PUR/methacrylic IPNs.<sup>16</sup>

## EXPERIMENTAL

### Materials

The PUR soft segment was polyoxypropylene glycol of a molar mass of 1025 (PPG1025, supplied by BDH). The hard segment was formed from the 1,1,3,3,-tetramethylxylene diisocyanate (*m*-TMXDI, kindly donated by Cytec) and the crosslinker trimethylol propane (TMP, supplied by Aldrich). Stannous octoate (SnOc, supplied by Sigma) was

used as the PUR catalyst. The acrylic component consisted of *n*-butyl methacrylate monomer (BMA, supplied by Aldrich) which was crosslinked with tetraethyleneglycol dimethacrylate (TEGDM, supplied by BDH) and initiated with azoisobutyronitrile (AIBN, supplied by BDH). The functionalized polystyrene latex particles were prepared using styrene (S, supplied by Aldrich) which was crosslinked with divinylbenzene (DVB, supplied by Aldrich) and initiated with 4,4'-azobis(4-cyanovaleric acid) (AVA, supplied by Aldrich). 2-Hydroxyethyl methacrylate (HEMA, supplied by Aldrich) was incorporated into the composite latex particles to provide surface functionality. Dodecyl sulfate sodium salt (DSS, supplied by Aldrich) was used as the emulsifier.

### Synthesis of PS and PS-HEMA Latex Particles

Crosslinked (1% DVB) polystyrene latex particles and functionalized particles containing HEMA (Fig. 1) were synthesized by emulsion polymerization. A styrene/divinylbenzene mixture was used to form a seed. Thus, 10% of the charge was added with the initiator after conditioning the water-emulsifier system for 1 h under nitrogen at 75°C. The remaining 90% monomer/crosslinker was fed in two stages over 4 h. A total of 80% was added over 3 h. After a further 30 min the remaining 10% with the HEMA was added. Finally, the latex was cryocrashed, filtered, and washed with hot water. The copolymerization ratios<sup>17</sup> for S and HEMA are  $r_1 = 0.57$  and  $r_2 = 0.65$  which indicates a tendency toward an alternating copolymerization. This, together with the low levels of HEMA, means that no substantial poly(HEMA) segments were formed. The latter was important since both HEMA and poly(HEMA) are strongly hydrophilic. The lattices were synthesized at overall HEMA levels of 0, 0.5, and 3 wt %.

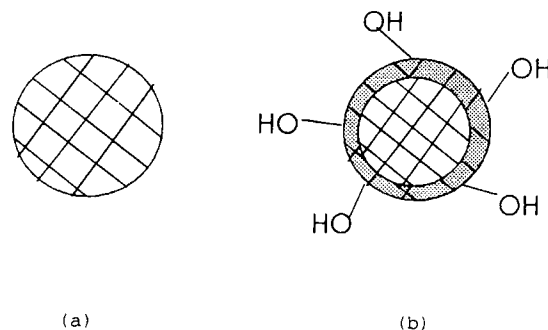


**Figure 1** Schematic representation of (a) the cross-linked polystyrene and (b) the structural HEMA-functionalized latex particles.

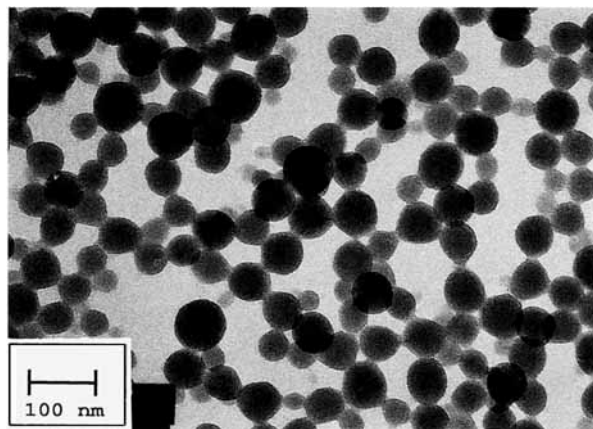


**Figure 2** TEM micrograph of structural PS-HEMA latex particles on a carbon film.

### Characterization of the Latex Particles

Photon correlation spectroscopy yielded particle sizes between 90 and 100 nm for the PS latex and

the PS-HEMA composite latex particles. Particle sizing via transmission electron microscopy (TEM) resulted in slightly lower values of 60–70 nm (Fig. 2). Diffuse reflectance infrared spectroscopy studies were conducted in order to confirm the incorporation of the HEMA into the PS latex particles (Fig. 3). Comparing the spectra obtained from the PS latex and the functional latex, the incorporation of HEMA is obvious from the presence of two additional absorption peaks. The hydroxyl peak appears at  $3458\text{ cm}^{-1}$  and the carbonyl stretching appears at  $1745\text{ cm}^{-1}$ . Modulated-temperature differential scanning calorimetry studies revealed a lower  $T_g$  for the functionalized particle than for the pure crosslinked PS latex (Fig. 4). The glass transition temperature of poly(HEMA)<sup>17</sup> is  $65^\circ\text{C}$ .

### IPN Preparation

The AIBN was dissolved in BMA and TEGDM. In a separate receptacle the TMP was melted and dis-

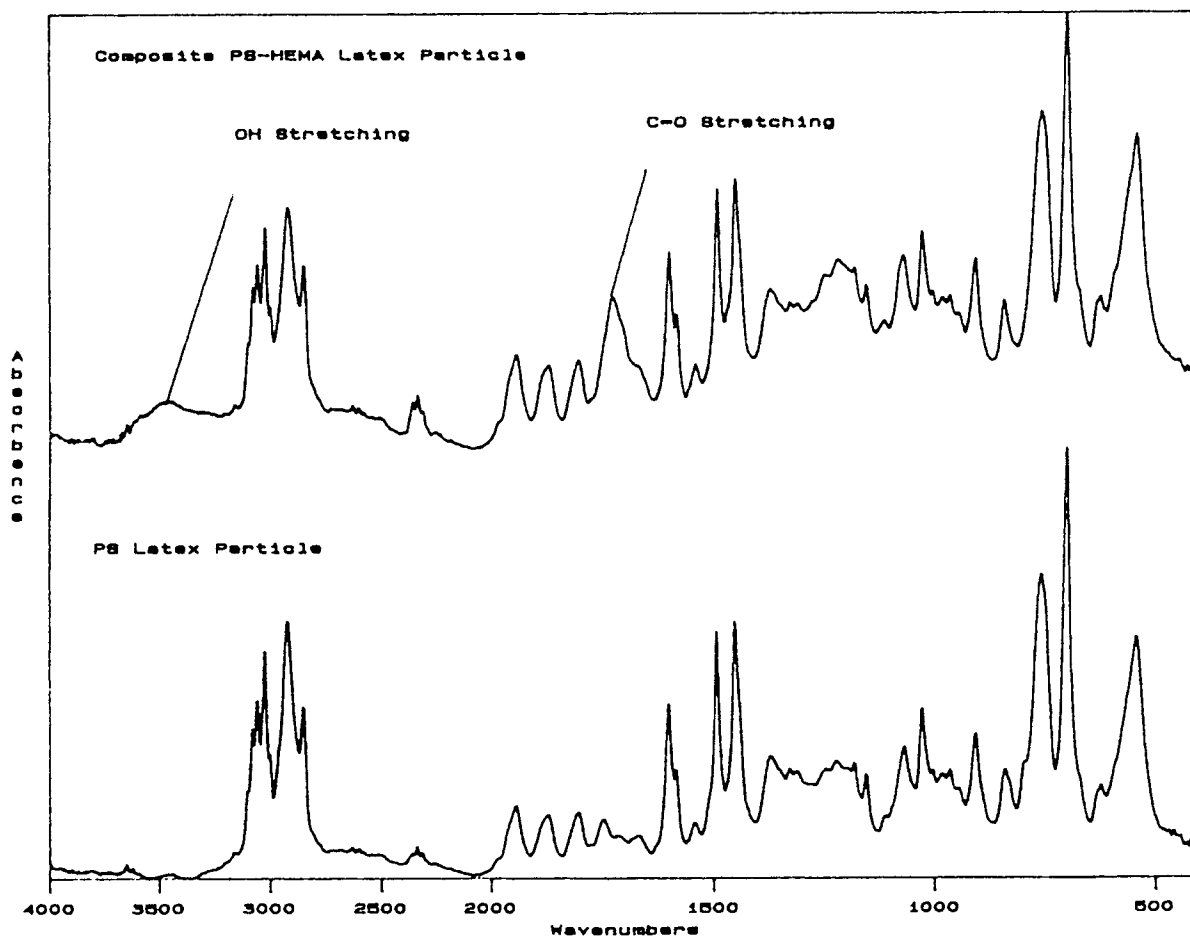


**Figure 3** Diffusion reflectance infrared spectra of the polystyrene- and the HEMA-functionalized polystyrene latex particles.

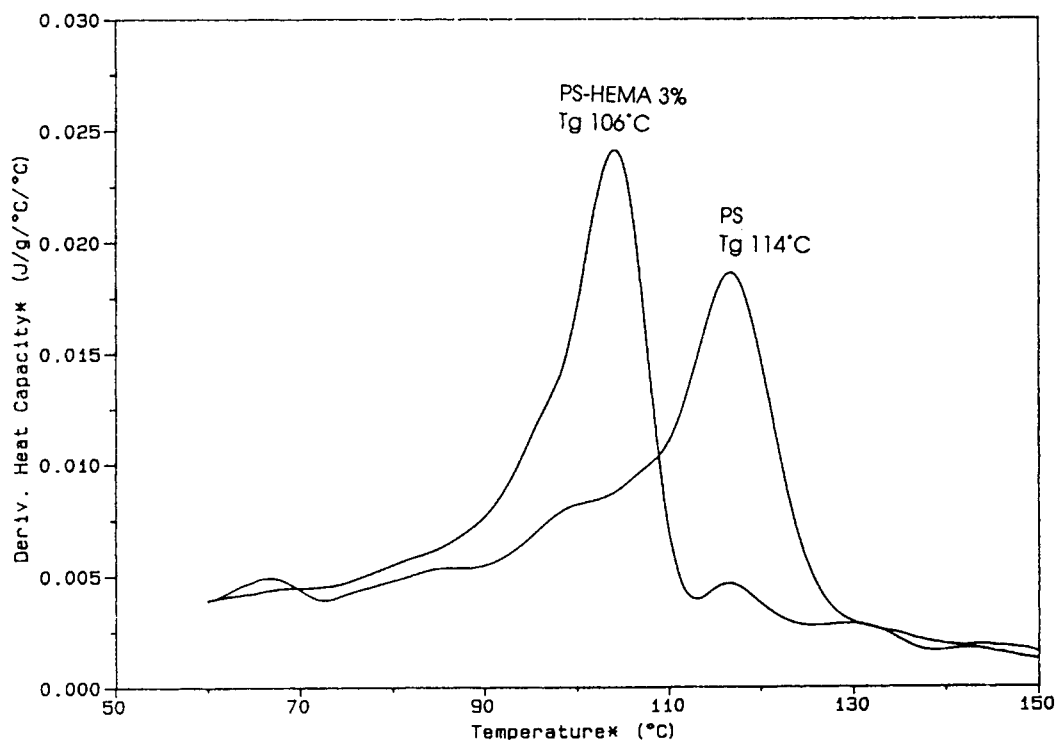


**Figure 4** Comparison of the differential of heat capacity versus temperature for the polystyrene- and the HEMA-functionalized latex particles.

solved in the PPG1025 at 60°C. At room temperature, the latex particles were dispersed in the polyol mixture using a high-speed mixer and the mixture was subsequently degassed. Both components were combined and the PUR catalyst and the *m*-TMXDI were added. For the preparation of the IPNs with the hydroxyl-functionalized latex particles, an additional stoichiometric amount of diisocyanate (*m*-TMXDI) was added to the original formulation in order to ascertain good network formation. The mixture was stirred at high speed for 5 min and then degassed for 1 min. Then, the mixture was cast into a stainless steel spring-loaded O-ring mold, which had been pretreated with release agent. The molds were placed into an open air oven for curing. The curing cycle consisted of three stages of 24 h at 60°C, 24 h at 80°C, and 24 h at 90°C. Four IPNs were synthesized at a 70 : 30 PUR/PBMA composition, one of which was the two-component PUR/PBMA IPN, whereas the remaining three contained 20 parts (17 wt %) of unfunctionalized and HEMA-functionalized (0.5 and 3 wt % of HEMA) PS latex particles.

#### Dynamic Mechanical Thermal Analysis

Rectangular test specimens were measured with a Polymer Laboratories MKII Dynamic Mechanical

Analyser in the single cantilever bending mode. The temperature program was run from -60 to 200°C using a heating ramp of 3°C per min at a fixed frequency of 10 Hz.

#### Tensile Testing

Stress-strain analyses were conducted using a Lloyd 2000R instrument equipped with a 500 N load cell. A crosshead speed of 50 mm/min was chosen. Small-size dumbbells with a gauge length of 30 mm were used in this study. Tests were conducted at  $23 \pm 1^\circ\text{C}$  and the values quoted are an average of four to five samples.

#### Hardness Measurements

Shore A hardness was determined using a Zwick model 3114 durometer. The testing was conducted at room temperature ( $23 \pm 1^\circ\text{C}$ ). Hardness values quoted are from an average of eight readings taken at random over the entire specimen surface.

#### TEM Micrographs

The elastomeric samples were embedded in epoxy resin and ultramicrotomed into 100 nm-thick sec-

tions. Staining was conducted for 48 h in a 2% osmium tetroxide solution. The electron micrographs were taken with a Jeol Jem 100 CX instrument using an accelerating voltage of 60 kV.

## RESULTS AND DISCUSSION

PUR and PBMA are a partially miscible polymer pair. Both contain groups that exhibit some polarity and their solubility parameters, determined by equilibrium swelling, are  $20.3 \text{ (J/cm}^3\text{)}^{1/2}$  for the PUR<sup>5</sup> and  $17.9 \text{ (J/cm}^3\text{)}^{1/2}$  for the PBMA.<sup>17</sup> The 70:30 PUR/PBMA IPN exhibited a broad transition peak with high  $\tan \delta$  values spanning both  $T_g$  transitions [Fig. 5 (a)].

However, its usefulness at temperatures higher than  $80^\circ\text{C}$  is very limited because of the significant softening of the material. At  $80^\circ\text{C}$ , the mechanical properties were poor which was manifested in the storage modulus curve approaching 0.1 MPa (Fig. 6).

Incorporation of the latex particles was conducted in order to increase the working temperature range of the damping material. The PS latex particles were swollen to some extent by the monomer/cross-

linker/initiator mixture and, thus, physically entangled with the methacrylic network. The incorporation of 20 parts of 1% DVB-crosslinked PS latex particles into the IPN sheet resulted in an additional peak at  $148^\circ\text{C}$  in the loss factor curve (Table I and Fig. 5).

The storage modulus curve now remained greater than 0.1 MPa until above  $160^\circ\text{C}$  (Fig. 6). Yet, the intertransition  $\tan \delta$  values were low (0.11) because of the poor compatibility between PBMA and PS. A better result was obtained with the hydroxyl-functionalized latex particles which were also incorporated at 20 parts by weight. In addition to the forced physical entanglement with the PBMA network, the hydroxyl functionality of the latex particles can also react with the m-TMXDI to become chemically linked with the PUR network, thus improving the system's miscibility. The latter could be observed by the inward shift of the PS transition from  $148$  to  $131^\circ\text{C}$  for the 0.5% and to  $118^\circ\text{C}$  for the 3% HEMA functionalized latex particles. Further, a clear increase of the  $\tan \delta$  value for the intertransition was observed from 0.11 for the system with the PS latex to 0.18 for both PS-HEMA functionalized latex particles. However, for a good

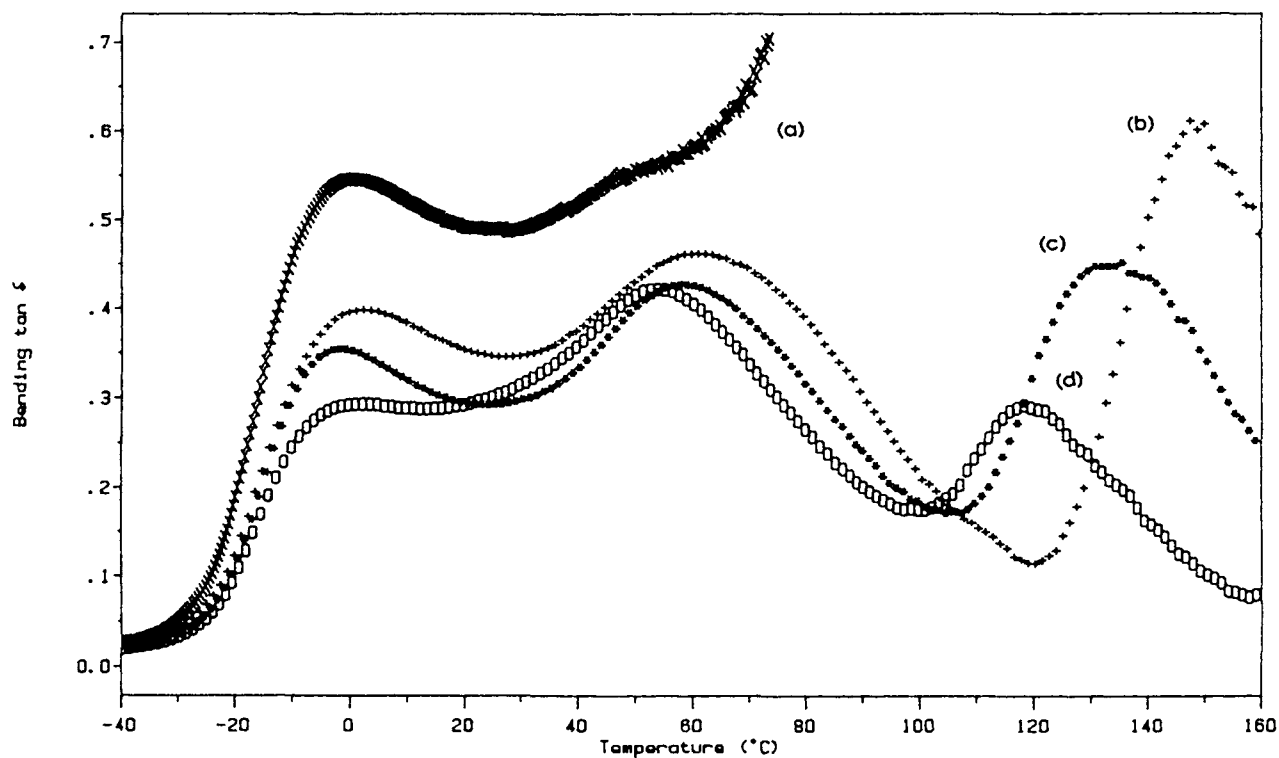


**Figure 5** Loss factor versus temperature data for the four IPNs. (a) PUR/PBMA, (b) PUR/PBMA/PS, (c) PUR/PBMA/PS-(HEMA 0.5%), and (d) PUR/PBMA/PS-(HEMA 3%).

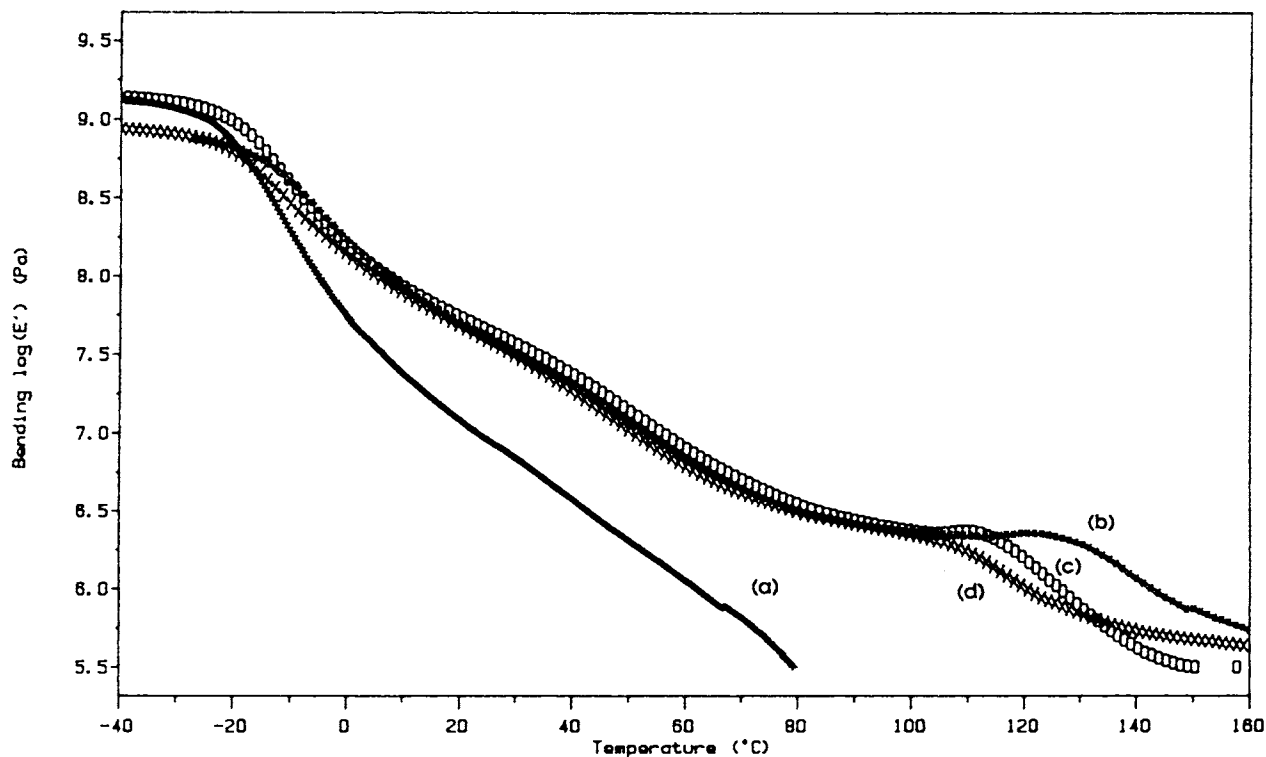


**Figure 6** Storage modulus versus temperature data for the four IPNs. (a) PUR/PBMA, (b) PUR/PBMA/PS, (c) PUR/PBMA/PS-(HEMA 0.5%), and (d) PUR/PBMA/PS-(HEMA 3%).

damping material, a  $\tan \delta$  value of 0.3<sup>18</sup> over the entire transition should be achieved. Therefore, further increasing the miscibility of the latex particles with the IPN is needed in order to obtain a good damping material. This may be achieved either by allowing more time for the PS latex particles to be swollen to a greater extent or by selecting a latex polymer with a solubility parameter closer to that of the methacrylic component. Work with polymethyl methacrylate latex particles is currently underway.

The area under the linear loss factor curve, TA, is an indication of the damping ability<sup>5,19</sup> of a material. In this study, it was difficult to compare the respective TA areas since the PUR/PBMA IPN became too soft at higher temperatures. Therefore, it was difficult to establish whether the PS latex particles acted as a filler and so imparted additional damping mechanisms into the material. Yet, from assessing the areas of the three-component IPNs, it could be noted that the incorporation of HEMA decreased the TA area. This can be attributed to the

**Table I** Dynamic Mechanical and Mechanical Properties of the IPNs

Samples	DMTA (10 Hz) $T_g$ ( $\tan \delta/^\circ\text{C}$ )	Ultimate Tensile Properties				
		Stress at Break (MPa)	Elongation at Break (%)	Young's Modulus (MPa)	Toughness (J)	Hardness Shore A
PUR/PBMA	PUR/PBMA/PS					
70/30 IPN	-2/ <sup>a</sup>	4.3	450	2	3.6	48
+ PS	-2/62/148	3.7	170	14	1.8	76
+ PS-HEMA 0.5%	-2/59/131	4.6	160	15	1.8	80
+ PS-HEMA 3%	-2/55/118	7.4	180	21	2.5	86

<sup>a</sup> Material became too soft for measurement.

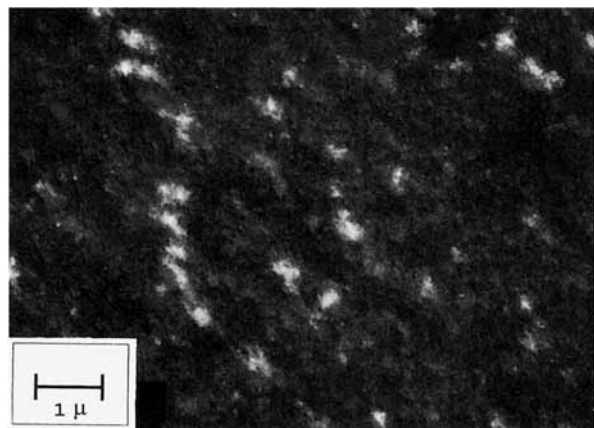


**Figure 7** TEM micrograph of the 70 : 30 PUR/PBMA IPN.

increase in crosslink density that was brought about by the functionalized latex particles. The pendent hydroxyl functionality of the HEMA-PS latex particles grafted onto the forming PUR network to form trifunctional crosslinks. These additional crosslinks decreased further the segmental mobility within the PUR network, resulting in a weakening of glass transition phenomenon which in turn showed itself in lower values for the loss factor,  $\tan \delta$ .

The tensile testing results are listed in Table I. Behavior typical of a filled polymer<sup>12,20</sup> was observed. An increase in Young's modulus is combined with a decrease in elongation and stress at break. The Young's modulus increased from 2 MPa for the PUR/PBMA IPN to 14, 15 and 21 MPa for the materials with the incorporated latex particles. The values for the elongation at break decreased considerably from 450% for the two-component IPN to less than 200% for all of the three-component IPNs. As a result, the toughness index also decreased by half from 3.6 J to around 2 J for the three PS-filled IPNs. For the stress at break, a more differentiated pattern was observed. The 70 : 30 PUR/PBMA IPN exhibited a greater value (4.3 MPa) than the IPN filled with 17 wt % PS latex particles (3.7 MPa). This indicated that the latex particles were not entangled to a great extent with the PBMA component. On introduction of HEMA into the PS latex particles, the stress at break values increased. With 0.5% HEMA incorporated in the PS latex, a slightly higher value of 4.6 MPa than for the two-component IPN was obtained. At 3% HEMA incorporation, the highest value by far with 7.4 MPa resulted for the stress at break. This indicated a better adhesion between the composite latex particles and the matrix which was caused by the formation of covalent bonds from the reaction of the hydroxyl groups with the isocyanate groups.

The Shore A hardness values increased strongly (Table I) with the incorporation of the functional latex particles from a value of 48 for the PUR/PBMA to 76 for the material with 17% PS latex particles. The functionalized particles resulted in even higher values with 80 for the particles with 0.5% HEMA and 86 for the material with 3% HEMA.

TEM studies were conducted to investigate the IPN morphology. For a better contrast, the samples were stained with osmium tetroxide which is known<sup>21</sup> to stain the polyurethane preferentially. For the PUR/PBMA IPN a fine morphology with very small phase domains was observed (Fig. 7).

Both larger PBMA-rich (white) domains of 200–300 nm and smaller domains of 40–70 nm in size were present. An even stronger indication of some degree of miscibility of the PUR/PBMA IPN than the small phase domain sizes is the blurred interface area. Various shades of gray indicated that the composition was changing only gradually, whereas in immiscible IPNs, such as for example PUR/PS IPNs,<sup>4</sup> clear-cut interfaces were observed.

The TEM micrographs of the three-component IPNs with the incorporated latex particles were all macroscopically similar in morphology and showed that the majority of the latex particles were not dispersed on an individual level. Agglomerates of the latex particles in the IPN matrix could be seen (Fig. 8).

The size of these agglomerates was in the order of 2–20  $\mu\text{m}$ , with a trend toward a smaller agglomerate size for the materials with the higher degree of functionalization in the latex particles. This trend toward smaller agglomerate sizes might be explained by the reaction of the forming PUR network during the 5-min mixing period with the hydroxyl-functionalized latex particles. Functionalized latex particles that were

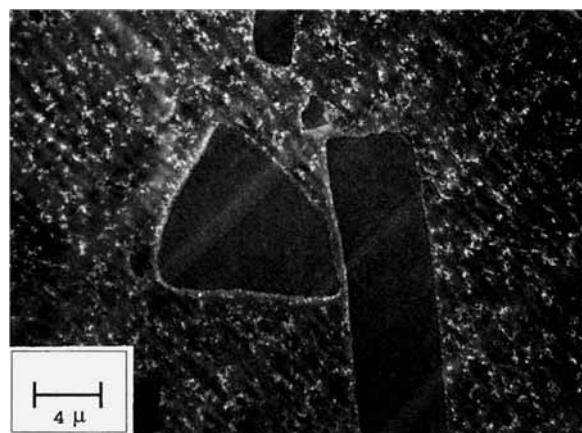


**Figure 8** TEM micrograph of the 70 : 30 PUR/PBMA IPN with 17% PS latex particles.

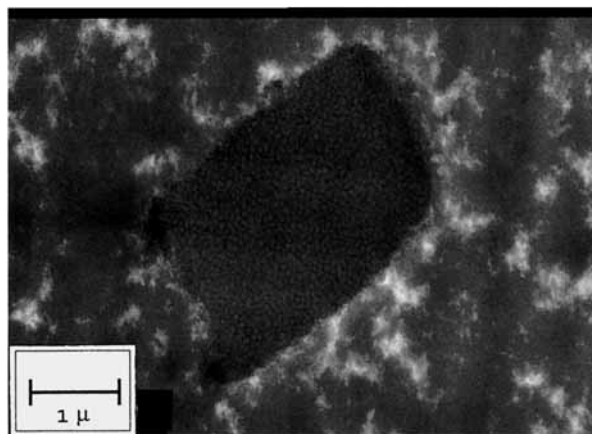


**Figure 9** TEM micrograph of the 70 : 30 PUR/PBMA IPN with 17% PS latex particles.

chemically linked with the forming PUR network are believed to be more prone to being torn out of the agglomerates, thus leading to the partial break-up of the latter. A micrograph of one PS latex particle agglomerate of 2–3  $\mu\text{m}$  which is surrounded by a PUR/PBMA matrix is shown in Figure 9.

The individual PS latex particles (white) can be seen in a dark agglomerate matrix. It was difficult to determine whether the agglomerate matrix was predominately composed of PUR or PBMA. Figure 9 indicates that the dark agglomerate matrix consisted mainly of osmium tetroxide-stained PUR. However, besides osmium tetroxide staining, the electron density (darkness) of the phases is also strongly influenced by the thickness of the ultrathin sample section. In this study, ultramicrotoming was conducted at room temperature. As a result, there was a pronounced difference in hardness of the PS-rich agglomerates and the surrounding matrix because of the high glass transition temperature of the PS. This might have led to a variation in section thickness which in turn could explain that, in other micrographs, the agglomerate matrix appeared lighter than the surrounding PUR/PBMA matrix.

Further, the TEM micrographs confirmed that the PS latex particles were not swollen to a great extent by the BMA monomer and the crosslinker. A comparison at the same magnification between the latex particles measured on a carbon film (Fig. 2) and the particles in an ultramicrotomed section of the three-component IPN with 17% PS latex particles (Fig. 10) showed them to be very similar in size.

At a high magnification of 75000 $\times$ , an additional difference between the incorporation of unfunctionalized and functionalized latex particles was noted. At a functionalization level of 3% HEMA in the PS

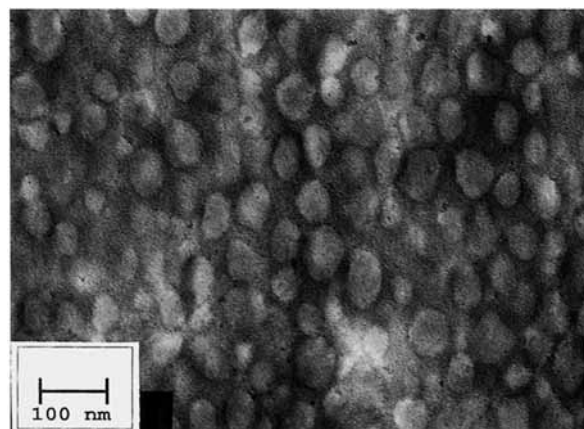


**Figure 10** TEM micrograph of the 70 : 30 PUR/PBMA IPN with 17% PS latex particles.

latex particles, numerous single functionalized PS particles were also observed outside the agglomerates in the PUR/PBMA matrix. Still, the interface between the PS latex particles agglomerates and the PUR/PBMA matrix was clearly visible, yet much less well defined for the material with the 3% HEMA-functionalized PS latex particle agglomerates. Figures 11 and 12 show similar interface regions of a material with unfunctionalized PS latex particles and with 3% HEMA-functionalized particles.

While in Figure 11 the single latex particles can be easily distinguished, much less well-defined interfaces within the agglomerate matrix were seen in Figure 12. This is believed to have stemmed from the reaction of the functionalized latex particles with the PUR network. The dark regions represent PUR-rich zones. Reaction between the forming PUR network and the functionalized latex particles led to the greater forced mixing seen in this micrograph.

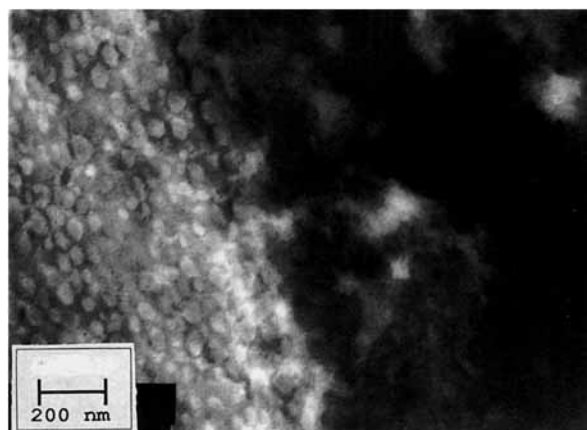


**Figure 11** TEM micrograph of the 70 : 30 PUR/PBMA IPN with 17% PS latex particles.



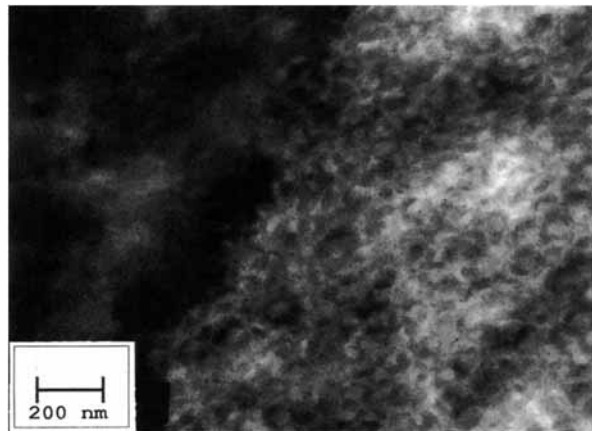


**Figure 12** TEM micrograph of the 70 : 30 PUR/PBMA IPN with 17% PS-HEMA 3% latex particles.

## CONCLUSIONS

The incorporation of 17 wt % composite PS latex particles significantly altered the property profile of a 70 : 30 PUR/PBMA IPN. The mechanical properties of the damping material were significantly improved by the incorporation of latex particles. This was evident in the higher values for the Young's modulus and the Shore A hardness. Also, increased values for the storage modulus in the higher temperature range from 80 to 140°C were found. Functional latex particles with hydroxyl functionality exhibited a better mixing with the microheterogeneous PUR/PBMA IPN than did unfunctionalized PS latex particles and, therefore, resulted in materials with better damping properties in the temperature range between 80 and 140°C. TEM micrographs confirmed the improved mixing of the functionalized latex particles. Further, it was observed that the latex particles were not dispersed on an individual level, but that agglomerates of a size between 2 and 20  $\mu\text{m}$  were formed.

## ACKNOWLEDGMENTS

One of the authors (F.-U. S.) acknowledges a grant from the German Academic Exchange Service, DAAD.

## REFERENCES

1. D. Klempner, L. Berkowski, in *Encyclopedia of Polymer Science and Engineering*, H. Mark, N. M. Bikales,

- C. G. Overberger, and G. Menges, Eds., Vol. 8, John Wiley & Sons, New York, 1988.
2. L. H. Sperling, in *Interpenetrating Polymer Networks*, ACS 239, D. Klempner, L. H. Sperling, and L. A. Utracki, Eds., American Chemical Society, Washington, DC, 1994.
3. L. H. Sperling, *Interpenetrating Polymer Networks and Related Materials*, Plenum Press, New York, 1981.
4. D. J. Hourston and F.-U. Schäfer, in Special Edition IPNs, *J. Polym. Adv. Technol.*, to appear.
5. D. J. Hourston and F.-U. Schäfer, *H. Perform. Polym.*, **8**, 19 (1996).
6. D. Klempner, K. C. Frisch, H. X. Xiao, and H. L. Frisch, *Polym. Eng. Sci.*, **25**, 488 (1985).
7. D. Klempner, K. C. Frisch, H. X. Xio, E. Cassidy, and H. L. Frisch, *Multicomponent Polymer Materials*, ACS 210, 1986.
8. D. Sophia, D. Klempner, Vahid Sendijarevic, B. Suthar, and K. C. Frisch, in *Interpenetrating Polymer Networks*, ACS 239, D. Klempner, L. H. Sperling, and L. A. Utracki, Eds., American Chemical Society, Washington, DC, 1994.
9. J. Wang, Y. Li, and X. Tang, in *Advances in IPNs*, Vol. IV, D. Klempner and K. C. Frisch, Eds., Technomic Publishing, Lancaster, PA, 1994.
10. P. A. Lovell, J. McDonald, D. E. J. Saunders, M. N. Sherratt, and R. J. Young, in *Toughend Plastics*, ACS 233, C. K. Riew and A. J. Kinloch, Eds., American Chemical Society, Washington, DC, 1993.
11. H.-J. Sue, E. I. Garcia-Meitin, D. M. Pickelman, and P. C. Yang, in *Toughend Plastics*, ACS 233, C. K. Riew and A. J. Kinloch, Eds., American Chemical Society, Washington, DC, 1993.
12. L. E. Nielson, *Mechanical Properties of Polymers and Composites*, Marcel Dekker, New York, 1974.
13. D. T. H. Wong and H. L. Williams, *J. Appl. Polym. Sci.*, **28**, 2187 (1983).
14. L. H. Sperling, in *Sound and Vibration Damping with Polymers*, R. D. Corsaro and L. H. Sperling, Eds., ACS Symp., Ser. 424, Washington, DC, 1990.
15. A. F. Chen and H. L. Williams, *J. Appl. Polym. Sci.*, **20**, 3387 (1976).
16. D. J. Hourston and F.-U. Schäfer, *Polymer*, to appear.
17. J. Brandrup and E. H. Immergut, Eds., *Polymer Handbook*, 3rd ed., Wiley, New York, 1989.
18. S. Yao, M. Jia, X. Yan, and Y. Wang, in *Polymers and Biomaterials*, H. Feng, Y. Han, and L. Huang, Eds., Elsevier B. V., 1991.
19. M. C. O. Chang, D. A. Thomas, and L. H. Sperling, *J. Appl. Polym. Sci., Polym. Phys.*, **26**, 1627, 1988.
20. A. W. Birley, B. Haworth, and J. Batchelor, *Physics of Plastics*, Hanser Publishers, Munich, 1991.
21. K. Kato, *Polym. Eng. Sci.*, **1**, 38, 1967.

Received October 30, 1995

Accepted January 4, 1996